THE JOURNAL OF PHYSICAL CHEMISTRY C

Article

pubs.acs.org/JPCC

Marked Increase in Hydrophobicity of Monolithic Carbon Cryogels via HCl Aging of Precursor Resorcinol–Formaldehyde Hydrogels: Application to 1-Butanol Recovery from Dilute Aqueous Solutions

Isao Ogino,* Sakai Kazuki, and Shin R. Mukai

Division of Chemical Process Engineering, Graduate School of Engineering, Hokkaido University, N13W8 Kita-ku, Sapporo 060-8628, Japan

ABSTRACT: Monolithic carbon cryogels having a honeycomb structure with pore openings a few tens of micrometers in diameter (Carbon MicroHoneycomb, CMH) were synthesized by directional freezing of precursor resorcinol–formaldehyde (RF) hydrogels and subsequent carbonization at temperatures ≥ 674 K. Aging of precursor RF monoliths with 1 N HCl aq. was found to markedly increase the hydrophobicity of the corresponding CMHs as characterized by water vapor adsorption experiments conducted at 298 K. Analysis of the water vapor adsorption data indicates that levels of hydrophobicity of CMHs are similar to those exhibited by other types of highly hydrophobic adsorbents, such as a coal-derived activated carbon and a defect-free pure silica zeolite Beta. HCl aging also drastically changes the porous structure of CMHs from microporous to micro/mesoporous as characterized by nitrogen adsorption/desorption experiments. Because of significantly enhanced hydrophobicity of CMHs as well as hierarchical pore structure (straight macropores connected with micro/mesopores), CMHs can readily separate 1-butanol molecules from a diluted aqueous solution at 310 K and demonstrate high capacities (up to ≈3.13 mol kg^{-1} at a 1-butanol concentration of 135 mM). The unique morphology of CMHs, consisting of straight macropores coupled with micro/mesopores embedded within honeycomb walls, and the highly hydrophobic surface properties offer future prospects of CMHs in various applications that require fast separation of hydrophobic molecules from a large volume of aqueous solutions.

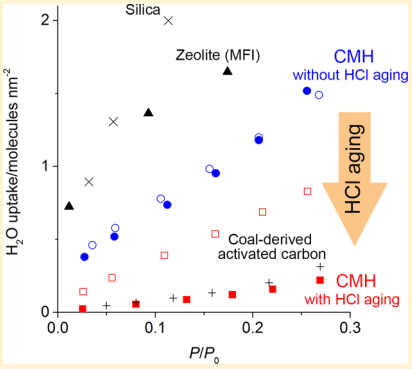

1. INTRODUCTION

Carbon gels, which are obtained through the carbonization of precursor organic gels, have attracted considerable attention for applications as energy storage materials,[1−8] separation media, and catalysts[9,10] because their porous properties can be tuned to match their usage by simply adjusting synthesis conditions. One of the most widely used precursor for carbon gels is a resorcinol–formaldehyde (RF) resin[11−13] that is synthesized by the polycondensation of resorcinol and formaldehyde in water using a base[11] or acid[14,15] catalyst. As in the case of sol–gel synthesis of silicate materials,[16] a wide variety of adjustable synthesis conditions, including the concentrations of monomers and a catalyst,[17,18] pH of the synthesis solution,[19] use of an organic template,[20] and drying conditions,[21] allow one to tailor the porous properties of resultant RF resins,[16,22,23] which ultimately determine the pore structure of the final carbonized materials. Further tuning of the pore structure of carbon gels can be accomplished by chemical or physical activation[13,24]

Another benefit of using RF resins as the precursor is the easiness of preparing structured materials. Preparations of various forms of carbon materials, such as monoliths, films, and discs, have been reported.[25−28] Mukai et al. reported the synthesis of monolithic carbon materials that have a honeycomb structure with pore openings a few tens of micrometers in diameter from carbonizing RF cryogels.[10,26,27,29,30] Because the pore openings of the aligned microchannels of such materials are in the micrometer range, these materials are called microhoneycombs (MHs). The aligned microchannels are formed by directional freezing of a precursor RF hydrogel using a cold bath, which forms straight ice rods a few tens of micrometers in diameters within the RF hydrogel network. Subsequent drying and carbonization yield microhoneycomb carbon cryogels. The unique morphology of MHs enables fast mass transfer of substrates by convection through straight channels and diffusion in short micropores present within the walls that form the channels. Furthermore, MHs cause significantly low resistance to a liquid flow.[10] Thus, MHs have prospective features as applications to separation media,[31] catalysts,[10] and catalyst supports.

In the synthesis of carbon gels from RF resins, aging (curing) of RF hydrogels in an acid solution is often employed after gelation to increase the strength of the resultant materials by increasing the cross-link density between polymer particles.[23] In our previous investigations, we found that aging MH-type RF resins in a diluted HCl aq. leads to the introduction of mesopores about 2.5 nm in diameter to the corresponding carbon microhoneycomb (CMH).[10] However, the investigation focused on the characterization of the porous properties. Here,

Received: December 30, 2013
Revised: March 11, 2014
Published: March 12, 2014

we found that HCl aging of precursor RF microhoneycombs significantly enhances the hydrophobicity of the corresponding CMHs. The high hydrophobicity of a series of CMHs is characterized by water vapor adsorption measurements, and the data are compared with those for a coal-derived activated carbon and high silica zeolites that are known to exhibit high hydrophobicity.[32]

To demonstrate the benefits of marked hydrophobicity as well as enhanced mesoporosity of CMHs via HCl aging, we tested CMHs as adsorbents for butanol recovery from an aqueous solution. Butanol produced via the traditional fermentation process (biobutanol) has attracted significant attention because butanol has fuel properties closely resembling those of gasoline and can be mixed with gasoline at any proportion.[33,34] The energy density of butanol is higher than that of ethanol and approximately 90% of that of gasoline. Furthermore, butanol is essentially noncorrosive, less volatile, and hygroscopic and has a higher flash point than ethanol, which makes it safer to handle.[34] Thus, butanol has prospects as a renewable energy source. One of the challenges associated with biobutanol production by fermentation processes (so-called ABE process) is the low butanol tolerance of bacteria, which limits the concentration of butanol to ≈1 wt % (≈135 mM) in the fermentation medium.[33] Recovery of 1-butanol from a dilute aqueous solution requires extensive energy. Separation of 1-butanol by distillation is cost- and energy-intensive because of the huge amount of water and the formation of an azeotrope from a mixture of 1-butanol and water.[35] Among various recovery techniques, pervaporation and adsorption were identified as the processes with the lowest energy consumption.[35] We demonstrate that CMHs show a high performance in 1-butanol uptake from diluted aqueous solutions in batch and flow adsorption systems.

2. EXPERIMENTAL SECTION

2.1. Materials. Resorcinol (99.0%), formaldehyde aqueous solution (36.0 wt % aqueous solution stabilized by methanol), sodium carbonate (99.8%), and 1 N HCl were used as received from Wako Pure Chemical Industries. A coal-derived steam activated carbon (Norit, GAC 1240W), MFI zeolite (JRC-Z5-90H, Catalysis Society of Japan, SiO_2/Al_2O_3 molar ratio = 90), and a macroporous polymeric adsorbent (Dowex Optipore, L-493, poly(styrene-*co*-divinylbenzene)) were used as reference adsorbents.

2.2. Synthesis of Resorcinol−Formaldehyde (RF) Monolith. RF monoliths were synthesized according to the literature.[10] Typically, a mixture of resorcinol (R), formaldehyde (F), sodium carbonate (C), and water (W) with the ratios among the four components being 1:2:0.02:61 was prepared in a polypropylene (PP) cup. The mixture was divided and charged to PP tubes (50 mm × 8 mm i.d.) that had been sealed at either end, and heated at 303 K for 20 h to allow the polycondensation reaction to proceed. After 20 h of the reaction, RF hydrogels were released from the PP molds and were washed with water. Then, each RF hydrogel was placed in a PP tube (13 mm i.d. × 125 mm), which was subsequently dipped into a liquid nitrogen bath at a rate of 60 mm/h. After the PP tube containing the frozen RF hydrogel was taken out of the liquid nitrogen bath, the RF hydrogel was immersed in 10 times their volume of *tert*-butyl alcohol (*t*-BuOH) for 1 day to exchange the water included in its structure with *t*-BuOH. This washing process was repeated three times using fresh *t*-BuOH each time. Aging a part of the RF hydrogels in HCl aq. was performed by immersing the frozen RF hydrogels in 20 mL of 1 N HCl aq. in a glass vial and keeping it there at room temperature for 1−20 days before washing with *t*-BuOH. The materials that had been washed with *t*-BuOH were freeze-dried at 263 K and carbonized as described in the next section. RF monolith samples are labeled as RFMH-DAY, where RFMH = RF MicroHoneycomb and DAY = treatment day(s) in 1 N HCl aq.

2.3. Carbonization of RF Monolith. Monolithic RF hydrogels prepared as in the preceding section were carbonized at 673−1073 K for 4 h in a tubular reactor in a nitrogen flow of 100 mL/min. Resultant samples are labeled as CMH-DAY-TEMP, where CMH = Carbonized RF MicroHoneycomb, DAY = treatment day(s) with 1 N HCl aq., and TEMP = carbonization temperature (K).

2.4. Characterization. The morphology of samples was characterized using a scanning electron microscope (SEM, JEOL Japan Inc., JSM-5410). The samples were mounted on a specimen stub using double-stick adhesive carbon tape. Nitrogen adsorption experiments were performed using an autoadsorber (BELSORP-mini II, Belsorp Japan) at liquid nitrogen temperature. In a typical measurement, an oven-dried measurement tube was weighed and then charged with approximately 50 mg of a sample. After the sample was pretreated in a flow of dry nitrogen at 523 K for 4 h, the tube containing the sample was sealed, weighed to determine the mass of the sample, and connected to the analysis port of the instrument. Micropore and total pore volumes were determined from N_2 uptakes at P/P_0 = 0.15 and 0.99, respectively. Mesopore size distributions and mesopore volumes were calculated by applying the Dollimore−Heal method to the adsorption isotherms. Vapor-phase adsorption of H_2O on carbon adsorbents including a commercially available activated carbon (Norit) was measured using an adsorption apparatus (BELMax, Belsorp Japan) at 298 K. In each experiment, approximately 50 mg of a carbonized material was placed in a sample tube, and was pretreated at 523 K for 4 h in a dynamic vacuum. High-silica zeolite (JRC-Z5-90H, silica/alumina molar ratio of 90) was pretreated at 523 K for 6 h in a dynamic vacuum. Solid-state ^{13}C CP/MAS NMR spectra were recorded on a Bruker MSL-300 at 75.3 MHz, a spinning rate of 6.0 kHz, and a contact time of 1 ms. Spectra of solid samples were collected in vacuum in transmission mode with a JASCO FT/IR-6100 Fourier transform spectrometer with a spectral resolution of 4 cm^{-1}.

2.5. Adsorption of 1-Butanol in a Batch Adsorption System. Adsorption isotherms of 1-butanol on CMHs were measured in a batch adsorption system at 310 K. A 6 mL glass vial was charged with 3 mL of 1-butanol aqueous solution at a specified concentration and 50 mg of an adsorbent, and then capped. The slurry was stirred vigorously using a stir bar in a thermostat bath set to 310 K for 24 h. After 24 h of stirring, an aliquot of the slurry was withdrawn through a syringe filter (SFNY013022, Membrane Solutions) using a disposable 1 mL PP syringe, and the resulting filtrate was analyzed using a gas chromatograph (GC-17A, Shimadzu Co. Ltd.) equipped with a capillary column (HR-1, 0.25 mm i.d., 25 m length, Shinwakako Co. Ltd.,) and an FID detector. Approximately ∼0.2 μL of the solution was injected into the column using the split mode option at a split ratio of 100:1. The injector and detector temperatures were set to 473 and 523 K, respectively. The oven temperature was held at 473 K. Equilibrium uptake of 1-butanol was calculated from the difference in the initial and final

dx.doi.org/10.1021/jp412781d | J. Phys. Chem. C 2014, 118, 6866−6872

concentrations by eq 1 assuming that the solution volume, V, was constant.

$$q = \frac{V(C_0 - C)}{m} \quad (1)$$

In eq 1, q represents the amount of 1-butanol uptake in mol (kg of adsorbent)$^{-1}$, V represents the solution volume in mL, C_0 represents the initial concentration of 1-butanol in mol L^{-1}, C represents the equilibrated concentration of 1-butanol in mol L^{-1}, and m represents the mass of the adsorbent in kg.

2.6. Adsorption of 1-Butanol from an Aqueous Solution in a Flow System. Adsorption of 1-butanol by a CMH was also conducted in a flow system. A CMH (17 mm in length and 8 mm in diameter) was cladded with a heat-shrinkable tube whose one end was connected to a feed line. An aqueous solution containing 135 mM of 1-butanol was fed to the CMH upward at a liquid hourly space velocity of 13 mL of butanol/(mL of CMH h^{-1}) from the bottom of the CMH that was held vertically in a thermostat bath set at 310 K. From time to time, an aliquot of the effluent was withdrawn by syringe and analyzed by the same procedure used in the batch system.

3. RESULTS AND DISCUSSION

3.1. Morphology of Synthesized RFMHs and Characterization of Them Using IR and ^{13}C CP MAS NMR. Various RFMHs were synthesized by varying the duration of the HCl treatment. A typically synthesized RFMH and carbonized sample have a cylinder shape, and the cross-sectional area of the cylinder shows aligned microchannels ≈ 100 μm in diameter (vide infra). The IR spectrum characterizing an RFMH-0 (sample without HCl aging) shows bands that can be assigned to modes typically found for an RF gel (Figure 1):[11] 2972, 2932, and 2870 cm^{-1} for C═H stretching

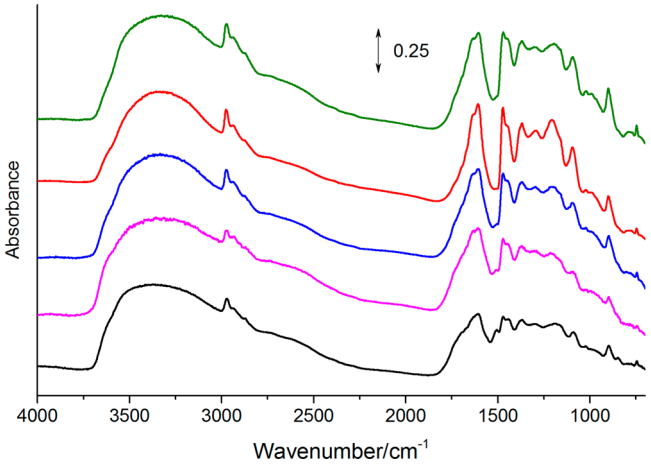

Figure 1. FT-IR spectra characterizing the RF monoliths treated with 1 N HCl for various periods of time: black, no HCl treatment (RFMH-0); magenta, 1 day (RFMH-1); blue, 4 days (RFMH-4); red, 8 days (RFMH-8); green, 20 days (RFMH-20).

modes; 1471 cm^{-1} for a C−H bending mode; 1614 and 1505 cm^{-1} for C═C stretching modes of aromatic rings; 3382 cm^{-1} for a O−H stretching mode; and 1210 and 1092 cm^{-1} for C−O−C stretching modes. A shoulder at approximately 1730 cm^{-1} indicates the formation of a small amount of carboxyl groups bonded to aromatic carbons[36] presumably formed via slight oxidation of RF gels by air during synthesis of the material. When HCl aging was included in the synthesis of RFMHs, a band at 1505 cm^{-1} disappeared and the absorbance of the shoulder at approximately 1730 cm^{-1} slightly decreased. Thus, the results indicate the consumption of carboxyl groups upon HCl aging.

To further investigate the effects of HCl treatment on the structure of RFMHs, ^{13}C CP MAS NMR characterization was performed for selected materials: RFMH-0, RFMH-4, and RFMH-20. All of the data show resonances that are consistent with an RF gel:[15,37] 153 ppm for aromatic carbons directly attached to OH groups, 134 ppm for aromatic carbons in the meta position relative to both phenolic carbons, 122 ppm for other aromatic carbons, 72 ppm for ether carbons, 61 ppm for aromatic carbons attached to OH groups, and 32 ppm for methylene carbons bridging two aromatic carbons (Figure 2).

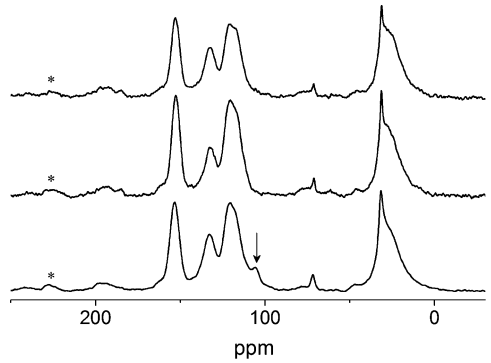

Figure 2. ^{13}C CP MAS NMR spectra characterizing the RF monoliths treated with 1 N HCl for various periods of time: bottom, no treatment (RFMH-0); middle, 4 days (RFMH-4); top, 20 days (RFMH-20). The arrow indicates a 105 ppm resonance that can be assigned to aromatic carbon between two phenolic carbons. The symbol ∗ indicates a spinning sideband.

The spectrum characterizing RFMH-0 shows a small peak at approximately 105 ppm,[37] which can be assigned to aromatic carbons between two phenolic carbons (ortho position relative to two phenolic carbons in resorcinol). This resonance was absent in the spectra characterizing the samples treated with 1 N HCl aq., indicating further reactions of aromatic carbons between two phenolic carbons. Although the IR data show the consumption of a fraction of carboxyl groups after HCl aging, resonances characteristic of carbonyl carbons at ∼190 ppm are virtually the same. It is assumed that the NMR spectroscopy was not sensitive enough to detect the small change that actually occurred.

In summary, the data show the successful synthesis of RFMHs. The results also indicate further reactions of aromatic carbons between two phenolic carbons and also consumption of a fraction of carboxyl groups by HCl aging. These changes appear to be rather small, but HCl aging causes substantial changes to the pore and surface properties as described in the next section.

3.2. Morphology and Porous Properties of Carbonized Monoliths. A carbonized material (CMH) typically obtained in this work retains the original cylinder shape of its parent RFMH (Figure 3), and SEM characterization of the cross-sectional area of the cylinder shows a honeycomb-like structure consisting of straight macropores ≈ 100 μm in diameter (Figure 3, inset). Height and diameter of the cylinder are adjustable by using PP tubes having different sizes for

dx.doi.org/10.1021/jp412781d | J. Phys. Chem. C 2014, 118, 6866−6872

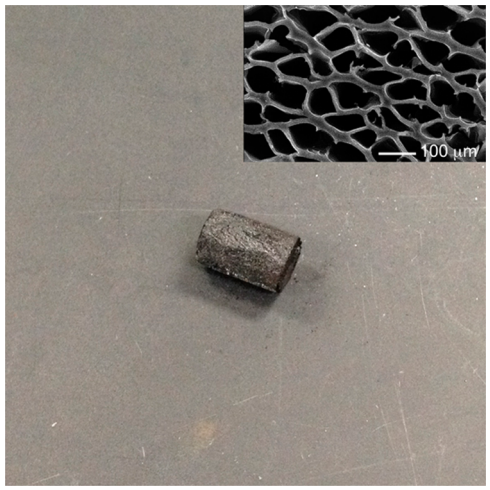

Figure 3. Photograph of a typical CMH synthesized in this work. The inset represents an SEM image of the cross-sectional area of the CMH.

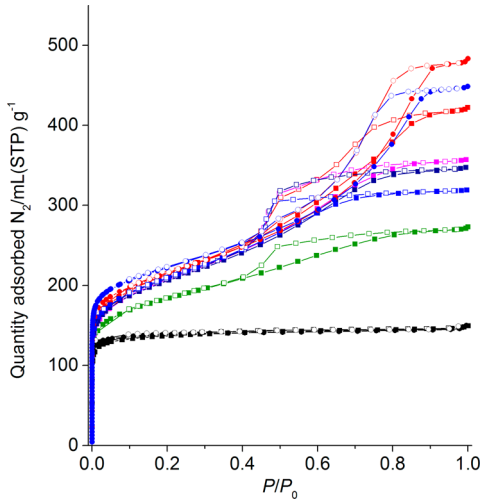

Figure 4. Nitrogen adsorption/desorption isotherms characterizing the following samples: CMH-0-1073 (solid black circle, open black circle); CMH-4-1073 (solid red circle, open red circle); CMH-20-1073 (solid blue circle, open blue circle); CMH-0-773 (solid black square, open black square); CMH-1-773 (solid green square, open green square); CMH-4-773 (solid red square, open red square); CMH-8-773 (solid pink square, open pink square); CMH-13-773 (solid navy square, open navy square); CMH-20-773 (solid blue square, open blue square). Solid and open symbols represent adsorption and desorption branches, respectively. The data for CMH-0-1073 and CMH-0-773 overlap each other.

synthesis. The picture in Figure 3 shows a CMH approximately 17 mm in length × 8 mm in diameter.

RF monoliths with and without HCl aging were carbonized at various temperatures, and their pore structures were characterized by nitrogen gas adsorption experiments. Carbonization of an RFMH-0 at 673 K (resultant material is CMH-0-673) gave essentially a nonporous material with V_{total} < 2 cm^3 g^{-1} (Table 1). Carbonization at 773 K (CMH-0-773) developed microporosity within the monolith walls, giving a type I isotherm (V_{micro} = 0.19 cm^3 g^{-1}, Table 1 and Figure 4). Further increase in the carbonization temperature to 1073 K resulted in the similar V_{micro}. However, when RF monoliths that had been treated with 1 N HCl aq. were carbonized, the resulting materials showed type IV isotherms (Figure 1), indicating that the treatment created mesoporosity within the carbon network.[10,38] Increasing time periods of HCl aging gradually increased micropore volumes, but mesopore volumes reached a maximum for samples aged with HCl for 4 days and decreased for longer aging times. Because the materials treated for 4 days (CMH-4-773 and CMH-4-1073) exhibit high micro- and mesopore volumes, we investigated their surface properties by H_2O vapor adsorption experiments.

Figure 5 shows water vapor adsorption isotherms characterizing CMHs. For comparison, the data of silica gel and high silica MFI zeolite (JRC-Z5-90H, Catalysis Society of Japan, SiO_2/Al_2O_3 molar ratio = 90) are also shown. The H_2O uptake data are normalized with respect to BET surface area to compare the hydrophobicity/hydrophilicity of materials having different surface areas. CMH-0-773 and CMH-0-1073 show similar H_2O uptakes. As BET surface areas of these two samples are also similar (Table 1), these data indicate that an increase in the carbonization temperature from 773 to 1073 K hardly increased the hydrophobicity of CMH. However, when HCl treatment was conducted before carbonization, the hydrophobicity of the corresponding CMH drastically increased (CMH-0-773 vs CMH-4-773 in Figure 5). Moreover, an increase in the carbonization temperature from 773 to 1073 K after HCl aging resulted in further enhancement in hydrophobicity (CMH-4-773 vs CMH-4-1073 in Figure 5).

To obtain more quantitative information about the effects of HCl aging on the hydrophobicity/hydrophilicity of CMHs, we used the method proposed by Pérez-Ramírez et al.[32] They used a simple method to evaluate hydrophilicity/hydrophobicity of high-silica zeolites. They carried out argon gas adsorption at

Table 1. Textural Properties of CMH Characterized by Nitrogen Gas Adsorption Experiments

sample	HCl aging[a]	carbonization temperature (K)	S_{BET} (m^2 g^{-1})	V_{micro}[b] (cm^3 g^{-1})	V_{meso}[c] (cm^3 g^{-1})	V_{total}[d] (cm^3 g^{-1})
CMH-0-673	none	673	2	<0.02		<0.02
CMH-0-773	none	773	536	0.19	<0.02	0.21
CMH-0-1073	none	1073	553	0.19	<0.02	0.21
CMH-1-773	1 day	773	674	0.24	0.18	0.42
CMH-4-773	4 days	773	776	0.29	0.30	0.59
CMH-8-773	8 days	773	749	0.30	0.25	0.55
CMH-13-773	13 days	773	762	0.30	0.24	0.54
CMH-20-773	20 days	773	758	0.31	0.18	0.49
CMH-4-1073	4 days	1073	778	0.29	0.38	0.67
CMH-20-1073	20 days	1073	814	0.22	0.23	0.45

[a]Time periods treated with 1 N HCl aq. [b]Calculated from adsorbed volume at P/P_0 = 0.15. [c]$V_{total} - V_{micro}$. [d]Calculatd from adsorbed volume at P/P_0 = 0.99.

dx.doi.org/10.1021/jp412781d | J. Phys. Chem. C 2014, 118, 6866−6872

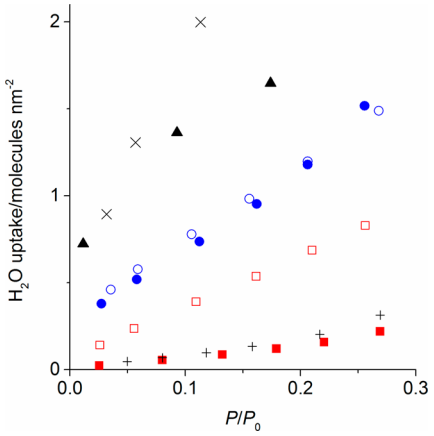

Figure 5. Vapor adsorption of water on pyrolyzed carbons at 298 K: silica gel (×), and MFI zeolite (SiO_2/Al_2O_3 ratio = 45) (black triangle), coal-derived activated carbon (Norit GAC 1240W) (+), CMH-0-773 (open blue circle), CMH-4-773 (open red square), CMH-0-1073 (solid blue circle), CMH-4-1073 (solid red square).

87.3 K and water vapor adsorption at 298 K, separately, on a set of MFI zeolites and calculated the ratios of water to argon uptakes at P/P_0 = 0.15 (defined as $x_{0.15}(H_2O)$ [%]).[32] At this relative pressure, micropore filling of argon seems to be complete. Therefore, the percentage ratio of water and argon uptakes gives the degree of pore filling by water molecules, which approximately measures the hydrophilicity of the surface of the zeolite (smaller ratios indicate higher hydrophobicity of the surface of zeolites). Using this method, they show that their materials (MFI zeolite, Si/Al atomic ratio ≈ 40) have $x_{0.15}(H_2O)$ = 21−33%. Our data for MFI zeolite (Si/Al atomic ratio of 45) are in line with their data, showing $x_{0.15}(H_2O)$ = 31% and indicate that nearly 1/3 of the micropores are filled with water molecules (Table 2). The $x_{0.15}(H_2O)$ values

Table 2. Water Vapor (V_{H_2O}) and Nitrogen Uptake (V_{N_2}) at P/P_0 = 0.15 and Calculated Ratio of $x_{0.15}(H_2O) = V_{H_2O}/V_{N_2} \times 100$

sample	V_{H_2O} ($cm^3\ g^{-1}$)	V_{N_2} ($cm^3\ g^{-1}$)	$x_{0.15}(H_2O)$ (%)
CMH-0-773	19.2	135	14
CMH-0-1073	18.5	137	13
CMH-1-773	15.3	177	9
CMH-4-773	14.6	204	7
CMH-8-773	13.8	197	7
CMH-13-773	14.3	197	7
CMH-20-773	11.7	200	6
CMH-4-1073	2.90	207	1
CMH-20-1073	3.30	215	2
Norit GAC 1240W	4.67	260	2
ZSM-5 (SiO_2/Al_2O_3 = 90)	35.4	114	31

calculated from the nitrogen and water vapor adsorption experiments for CMHs are listed in Table 2. The $x_{0.15}(H_2O)$ values of CMH-0-773 and CMH-0-1073 show that about 13% of micropores were filled with water molecules. Addition of HCl aging to the synthesis process of RF monoliths, which were subsequently carbonized at 773 K, resulted in ∼50% reduction of $x_{0.15}(H_2O)$ to ∼7%. The reduction of $x_{0.15}(H_2O)$ was pronounced for the material carbonized at 1073 K, showing significantly low $x_{0.15}(H_2O)$ values (≤2%). Hydrophobicity for these materials seems similar to that of an activated carbon (Norit, GAC 1240W) and also that reported for a pure silica zeolite Beta that is defect-free. Gounder and Davis reported the synthesis of defect-free pure silica zeolite Beta using fluoride media.[39] Calculation of the degree of pore filling by water molecules from their data (reported at P/P_0 = 0.20) gives the degree of pore filling of 1% (calculated as (0.0022 cm^3 (STP)/g of water)/(0.19 cm^3/g of micropore volume) × 100 = 1% from Table 1 reported in the literature[39]).

In summary, our data show that HCl aging of RFMHs drastically increases the hydrophobicity of the corresponding CMHs to levels exhibited by defect-free pure silica zeolite Beta. Because of the presence of relatively large mesopore volumes in CMHs, they are expected to exhibit high performance in adsorption of hydrophobic molecules from aqueous solutions. Thus, we evaluated their ability of 1-butanol recovery from diluted aqueous solutions as described in the next section.

3.3. Adsorption of 1-Butanol in a Batch System.

Adsorption of 1-butanol on various adsorbents was carried out at 310 K. Figure 6 shows the adsorption isotherms. For

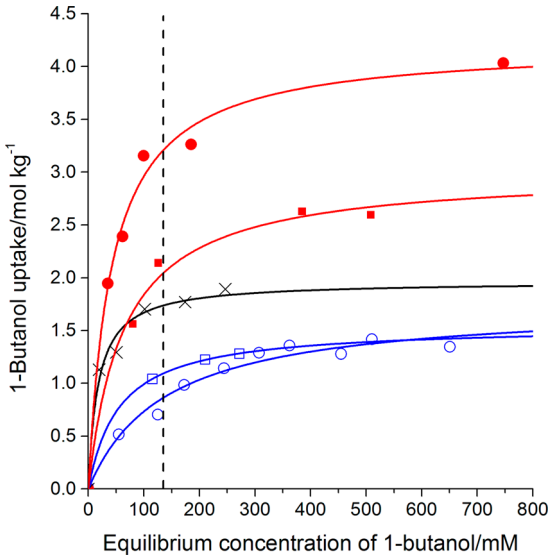

Figure 6. Adsorption isotherms of 1-butanol on CMHs and a high silica MFI zeolite at 310 K: CMH-0-773 (open blue square), CMH-4-773 (solid red square), CMH-0-1073 (open blue circle), CMH-4-1073 (solid red circle), MFI zeolite (SiO_2/Al_2O_3 = 90) (×). The dashed line indicates the upper limit of butanol concentration in biobutanol production.

comparison, the data for a high silica zeolite were included. All data can be well-represented by the Langmuir eq 2

$$q = \frac{q_m KC}{1 + KC} \quad (2)$$

where q represents the amount of 1-butanol uptake in mol (kg of adsorbent)$^{-1}$, q_m represents the maximum loading corresponding to complete surface coverage (monolayer coverage for ideal Langmuir adsorption) in mol (kg of adsorbent)$^{-1}$, K represents the adsorption-equilibrium constant in mM^{-1}, and C represents the equilibrium concentration of 1-butanol in mM. The maximum 1-butanol loading for ZSM-5 zeolite (2.04 mol kg^{-1}, 0.15 g of butanol (g of zeolite)$^{-1}$) is similar to that reported by Saravanan et al. with their ZSM-5 (CBV20814, Zeolyst).[40]

dx.doi.org/10.1021/jp412781d | J. Phys. Chem. C 2014, 118, 6866−6872

This value corresponds to four butanol molecules per unit cell of an MFI zeolite and thus appears to be reasonable. Both CMH-0-773 and CMH-0-1073 show similar butanol isotherms, consistent with their similar pore structure and surface hydrophobicity. CMH-4-773 shows higher amounts of 1-butanol than these materials probably because of its larger pore volumes and higher hydrophobicity. The 1-butanol adsorption density of CMH-4-773, which was calculated by dividing the total amount of 1-butanol uptake by its BET surface area, shows an ≈50% increase when compared to that of CMH-0-773 (Table 3), consistent with the higher hydrophobicity of the

Table 3. Results from 1-Butanol Adsorption on CMHs or an MFI Zeolite

sample	q_m[a] (mol kg^{-1})	q_{135}[b] (mol kg^{-1})	N_{BuOH}[c] (nm^{-2})
CMH-0-773	1.37	1.17	1.5
CMH-0-1073	1.68	0.875	1.8
CMH-4-773	2.94	2.06	2.3
CMH-4-1073	4.27	3.13	3.2
ZSM-5	2.04	1.75	2.2

[a]Maximum 1-butanol uptake. [b]1-Butanol uptake at 135 mM. [c]1-Butanol uptake per unit surface area.

former sample. Butanol uptake at the equilibrium concentration of 135 mM (q_{135}), which is the upper limit of concentration in biobutanol recovery, is similar to that of the high silica zeolite (2.06 mol kg^{-1} for CMH-4-773 and 1.75 mol kg^{-1} for the zeolite, Table 3). CMH-4-1073 shows even higher amounts of 1-butanol uptake and shows a high q_{135} of 3.13 mol kg^{-1}, approaching the value reported for one of the best commercially available adsorbents (Dowex Optipore, L-493, poly(styrene-*co*-divinylbenzene), BET surface area = 1100 m^2 g^{-1}), which shows q_{135} = 4.10 mol kg^{-1} as reported by Prather et al.[41] CMH-4-1073 shows the largest average number of 1-butanol molecules per unit surface area (≈3 molecules nm^{-2}). This value corresponds to 0.3 nm^2 per molecule. The effective cross-sectional area of a 1-butanol molecule is approximately 0.2 nm^2 (calculated from the kinetic diameter 0.5 nm[42]). If each butanol molecule is adsorbed vertically on the surface of carbon with its methyl group pointing to the surface, three 1-butanol molecules nm^{-2} approaches the upper limit for monolayer coverage. Carbon adsorbents have an advantage to polymer adsorbents because the operating temperature limits for the latter adsorbents are relatively low (e.g., 383 K for L-493[43]). In summary, HCl aging appears to have positive effects on the performance of a CMH for 1-butanol adsorption and CMH-4-1073 shows a high 1-butanol uptake.

3.4. Adsorption of 1-Butanol in a Flow System. Adsorption of 1-butanol was also carried out in a flow system. Figure 7 shows the breakthrough curve of the CMH-4-1073. The material shows a sigmoidal curve typically found in breakthrough experiments. The 1-butanol loadings at 10% and 100% breakthroughs were calculated as 0.10 and 0.74 g/g of CMH, which are both higher than those of highly siliceous zeolite reported in the literature.[40] Thus, the results show that CMH functions effectively as an adsorbent in flow systems.

4. CONCLUSIONS

A series of monolithic carbon cryogels having a micro-honeycomb structure (CMH) were synthesized by directional freezing of resorcinol−formaldehyde hydrogels, followed by freeze-drying and partial carbonization at elevated temperatures. Aging of RF monoliths (precarbonized material) using 1 N HCl aq. was found to markedly increase the hydrophobicity of the corresponding CMHs. HCl aging also increased micropore volumes and introduced mesoporosity to the carbon network. H_2O vapor adsorption experiments and analysis of the resultant data show that the CMH treated with 1 N HCl aq. for 4 days, followed by carbonization at 1073 K, exhibits a highly hydrophobic surface that approaches levels of other highly hydrophobic adsorbents, such as an activated carbon and a defect-free pure silica zeolite Beta. Because of their high hydrophobicity as well as their unique hierarchical pore structure, CMHs show high 1-butanol uptakes from diluted aqueous solutions both in batch and flow systems. Thus, these data indicate that CMHs will find various applications that require fast separation of hydrophobic molecules from a large volume of aqueous solutions. Furthermore, the relatively simple treatment of HCl aging would be applicable to other types of carbons derived from phenolic resins to form highly hydrophobic carbons.

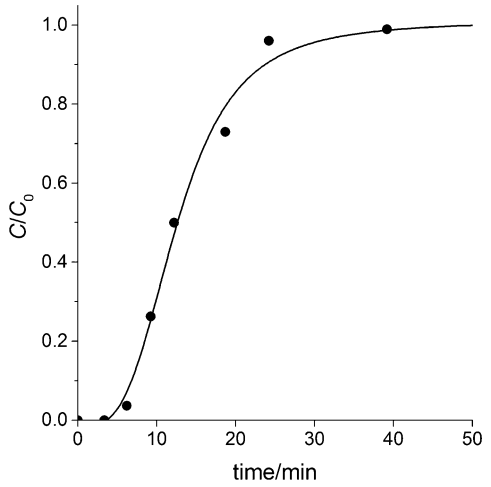

Figure 7. Breakthrough curve of 1-butanol in the CMH-4-1073.

AUTHOR INFORMATION

Corresponding Author

*Tel: +81 (11) 706-6591. E-mail: iogino@eng.hokudai.ac.jp.

Notes

The authors declare no competing financial interest.

REFERENCES

(1) Pandolfo, A. G.; Hollenkamp, A. F. Carbon Properties and Their Role in Supercapacitors. *J. Power Sources* **2006**, *157*, 11−27.

(2) Pröbstle, H.; Wiener, M.; Fricke, J. Carbon Aerogels for Electrochemical Double Layer Capacitors. *J. Porous Mater.* **2003**, *10*, 213−222.

(3) Pekala, R. W.; Farmer, J. C.; Alviso, C. T.; Tran, T. D.; Mayer, S. T.; Miller, J. M.; Dunn, B. Carbon Aerogels for Electrochemical Applications. *J. Non-Cryst. Solids* **1998**, *225*, 74−80.

(4) Nishihara, H.; Kyotani, T. Templated Nanocarbons for Energy Storage. *Adv. Mater. (Weinheim, Ger.)* **2012**, *24*, 4473−4498.

(5) Frackowiak, E.; Béguin, F. Carbon Materials for the Electrochemical Storage of Energy in Capacitors. *Carbon* **2001**, *39*, 937−950.

(6) Li, J.; Wang, X.; Huang, Q.; Gamboa, S.; Sebastian, P. J. Studies on Preparation and Performances of Carbon Aerogel Electrodes for the Application of Supercapacitor. *J. Power Sources* **2006**, *158*, 784−788.

(7) Calvo, E. G.; Lufrano, F.; Staiti, P.; Brigandì, A.; Arenillas, A.; Menéndez, J. A. Optimizing the Electrochemical Performance of

Aqueous Symmetric Supercapacitors Based on an Activated Carbon Xerogel. *J. Power Sources* **2013**, *241*, 776−782.
(8) Macías, C.; Haro, M.; Parra, J. B.; Rasines, G.; Ania, C. O. Carbon Black Directed Synthesis of Ultrahigh Mesoporous Carbon Aerogels. *Carbon* **2013**, *63*, 487−497.
(9) Moreno-Castilla, C.; Maldonado-Hódar, F. J. Carbon Aerogels for Catalysis Applications: An Overview. *Carbon* **2005**, *43*, 455−465.
(10) Murakami, K.; Satoh, Y.; Ogino, I.; Mukai, S. R. Synthesis of a Monolithic Carbon-Based Acid Catalyst with a Honeycomb Structure for Flow Reaction Systems. *Ind. Eng. Chem. Res.* **2013**, *52*, 15372−15376.
(11) Pekala, R. W. Organic Aerogels from the Polycondensation of Resorcinol with Formaldehyde. *J. Mater. Sci.* **1989**, *24*, 3221−3227.
(12) Pekala, R. W.; Alviso, C. T.; Kong, F. M.; Hulsey, S. S. Aerogels Derived from Multifunctional Organic Monomers. *J. Non-Cryst. Solids* **1992**, *145*, 90−98.
(13) Hanzawa, Y.; Kaneko, K.; Pekala, R. W.; Dresselhaus, M. S. Activated Carbon Aerogels. *Langmuir* **1996**, *12*, 6167−6169.
(14) Brandt, R.; Petricevic, R.; Pröbstle, H.; Fricke, J. Acetic Acid Catalyzed Carbon Aerogels. *J. Porous Mater.* **2003**, *10*, 171−178.
(15) Mulik, S.; Sotiriou-Leventis, C.; Leventis, N. Time-Efficient Acid-Catalyzed Synthesis of Resorcinol−Formaldehyde Aerogels. *Chem. Mater.* **2007**, *19*, 6138−6144.
(16) Pierre, A. C.; Pajonk, G. M. Chemistry of Aerogels and Their Applications. *Chem. Rev.* **2002**, *102*, 4243−4266.
(17) Saliger, R.; Bock, V.; Petricevic, R.; Tillotson, T.; Geis, S.; Fricke, J. Carbon Aerogels from Dilute Catalysis of Resorcinol with Formaldehyde. *J. Non-Cryst. Solids* **1997**, *221*, 144−150.
(18) Horikawa, T.; Hayashi, J.; Muroyama, K. Controllability of Pore Characteristics of Resorcinol−Formaldehyde Carbon Aerogel. *Carbon* **2004**, *42*, 1625−1633.
(19) Lin, C.; Ritter, J. A. Effect of Synthesis pH on the Structure of Carbon Xerogels. *Carbon* **1997**, *35*, 1271−1278.
(20) Wang, X.; Liang, C.; Dai, S. Facile Synthesis of Ordered Mesoporous Carbons with High Thermal Stability by Self-Assembly of Resorcinol−Formaldehyde and Block Copolymers under Highly Acidic Conditions. *Langmuir* **2008**, *24*, 7500−7505.
(21) Tamon, H.; Ishizaka, H.; Yamamoto, T.; Suzuki, T. Preparation of Mesoporous Carbon by Freeze Drying. *Carbon* **1999**, *37*, 2049−2055.
(22) Bock, V.; Emmerling, A.; Fricke, J. High Surface Area Carbon Aerogels for Supercapacitors. *J. Non-Cryst. Solids* **1998**, *225*, 69−73.
(23) Al-Muhtaseb, S. A.; Ritter, J. A.; Al-Muhtaseb, S. A.; Ritter, J. A. Preparation and Properties of Resorcinol−Formaldehyde Organic and Carbon Gels. *Adv. Mater. (Weinheim, Ger.)* **2003**, *15*, 101−114.
(24) Baumann, T. F.; Worsley, M. A.; Han, T. Y.-J.; Satcher, J. H., Jr. High Surface Area Carbon Aerogel Monoliths with Hierarchical Porosity. *J. Non-Cryst. Solids* **2008**, *354*, 3513−3515.
(25) Zapata-Benabithe, Z.; Carrasco-Marín, F.; de Vicente, J.; Moreno-Castilla, C. Carbon Xerogel Microspheres and Monoliths from Resorcinol−Formaldehyde Mixtures with Varying Dilution Ratios: Preparation, Surface Characteristics, and Electrochemical Double-Layer Capacitances. *Langmuir* **2013**, *29*, 6166−6173.
(26) Nishihara, H.; Mukai, S. R.; Tamon, H. Preparation of Resorcinol−Formaldehyde Carbon Cryogel Microhoneycombs. *Carbon* **2004**, *42*, 899−901.
(27) Mukai, S. R.; Nishihara, H.; Yoshida, T.; Taniguchi, K.; Tamon, H. Morphology of Resorcinol−Formaldehyde Gels Obtained through Ice-Templating. *Carbon* **2005**, *43*, 1563−1565.
(28) Morales-Torres, S.; Maldonado-Hódar, F. J.; Pérez-Cadenas, A. F.; Carrasco-Marín, F. Structural Characterization of Carbon Xerogels: From Film to Monolith. *Microporous Mesoporous Mater.* **2012**, *153*, 24−29.
(29) Mukai, S. R.; Nishihara, H.; Tamon, H. Morphology Maps of Ice-Templated Silica Gels Derived from Silica Hydrogels and Hydrosols. *Microporous Mesoporous Mater.* **2008**, *116*, 166−170.
(30) Mukai, S. R.; Tamitsuji, C.; Nishihara, H.; Tamon, H. Preparation of Mesoporous Carbon Gels from an Inexpensive Combination of Phenol and Formaldehyde. *Carbon* **2005**, *43*, 2628−2630.
(31) Mukai, S. R.; Satoh, Y. Development of a Strong Acid Ion Exchange Resin with a Monolithic Microhoneycomb Structure Using the Ice Templating Method. *Ind. Eng. Chem. Res.* **2010**, *49*, 10438−10441.
(32) Thommes, M.; Mitchell, S.; Pérez-Ramírez, J. Surface and Pore Structure Assessment of Hierarchical MFI Zeolites by Advanced Water and Argon Sorption Studies. *J. Phys. Chem. C* **2012**, *116*, 18816−18823.
(33) Garcia, V.; Pakkila, J.; Ojamo, H.; Muurinen, E.; Keiski, R. L. Challenges in Biobutanol Production: How to Improve the Efficiency? *Renewable Sustainable Energy Rev.* **2011**, *15*, 964−980.
(34) Jin, C.; Yao, M.; Liu, H.; Lee, C.-f. F.; Ji, J. Progress in the Production and Application of n-Butanol as a Biofuel. *Renewable Sustainable Energy Rev.* **2011**, *15*, 4080−4106.
(35) Oudshoorn, A.; van der Wielen, L. A. M.; Straathof, A. J. J. Assessment of Options for Selective 1-Butanol Recovery from Aqueous Solution. *Ind. Eng. Chem. Res.* **2009**, *48*, 7325−7336.
(36) Fanning, P. E.; Vannice, M. A. A Drifts Study of the Formation of Surface Groups on Carbon by Oxidation. *Carbon* **1993**, *31*, 721−730.
(37) Werstler, D. D. Quantitative ^{13}C n.m.r. Characterization of Aqueous Formaldehyde Resins: 2. Resorcinol-Formaldehyde Resins. *Polymer* **1986**, *27*, 757−764.
(38) Kraiwattanawong, K.; Mukai, S. R.; Tamon, H.; Lothongkum, A. W. Improvement of Mesoporosity of Carbon Cryogels by Acid Treatment of Hydrogels. *Microporous Mesoporous Mater.* **2008**, *115*, 432−439.
(39) Gounder, R.; Davis, M. E. Beyond Shape Selective Catalysis with Zeolites: Hydrophobic Void Spaces in Zeolites Enable Catalysis in Liquid Water. *AIChE J.* **2013**, *59*, 3349−3358.
(40) Saravanan, V.; Waijers, D. A.; Ziari, M.; Noordermeer, M. A. Recovery of 1-Butanol from Aqueous Solutions Using Zeolite ZSM-5 with a High Si/Al Ratio; Suitability of a Column Process for Industrial Applications. *Biochem. Eng. J.* **2010**, *49*, 33−39.
(41) Nielsen, D. R.; Amarasiriwardena, G. S.; Prather, K. L. J. Predicting the Adsorption of Second Generation Biofuels by Polymeric Resins with Applications for in Situ Product Recovery (ISPR). *Bioresour. Technol.* **2010**, *101*, 2762−2769.
(42) Wu, H.; Gong, Q.; Olson, D. H.; Li, J. Commensurate Adsorption of Hydrocarbons and Alcohols in Microporous Metal Organic Frameworks. *Chem. Rev.* **2012**, *112*, 836−868.
(43) Levario, T. J.; Dai, M.; Yuan, W.; Vogt, B. D.; Nielsen, D. R. Rapid Adsorption of Alcohol Biofuels by High Surface Area Mesoporous Carbons. *Microporous Mesoporous Mater.* **2012**, *148*, 107−114.